MOUNTAIN-PLAINS CONSORTIUM

MPC 21-447 | Y. Huang, P. Lu, R. Bridgelall, X. Yang and Y. Ren

INFRASTRUCTURE SAFETY
SUPPORT SYSTEM FOR
SMART CITIES WITH
AUTONOMOUS VEHICLES

Smart Sensing
& Smart City
Analysis

MOUNTAIN-PLAINS
CONSORTIUM REGION 8

Technical Report Documentation Page

1. Report No. MPC-547	2. Government Accession No.	3. Recipient's Catalog No.
4. Title and Subtitle Infrastructure Safety Support System for Smart Cities with Autonomous Vehicles		5. Report Date December 2021
		6. Performing Organization Code
7. Author(s) Dr. Y. Huang, Dr. R. Bridgelall, Dr. P. Lu, X. Yang, Y. Ren		8. Performing Organization Report No. MPC 21-447
9. Performing Organization Name and Address North Dakota State University Upper Great Plains Transportation Institute 418 Quentin Burdick Building Fargo, ND 58102		10. Work Unit No. (TRAIS)
		11. Contract or Grant No.
12. Sponsoring Agency Name and Address Mountain-Plains Consortium North Dakota State University PO Box 6050, Fargo, ND 58108		13. Type of Report and Period Covered Final Report
		14. Sponsoring Agency Code

16. Abstract

Driverless vehicles must be self-aware to make learned and ethical decisions to avoid crashes in multimodal and diverse settings. This proposed effort will develop an *Infrastructure Safety Support System* by embedding V2I enabled sensor networks into the transportation infrastructure to provide autonomous vehicles and human drivers with inputs to improve their decision making when obvious decisions may not possible. The research objectives of this project are to:

- Develop an infrastructure embedded sensor network to provide real-time traffic and road condition information such as traffic volume (e.g. ADT, peak-hour traffic), traffic composition (vehicle classification), vehicle speed, dynamic weight via weigh-in-motion (WIM), traffic density, traffic flow rate, road roughness, and other data;
- Develop algorithms that the infrastructure safety support system will use to process the sensor-based real-time traffic data and pavement conditions to support the decision-making processes of autonomous vehicles such as driving speed and safe vehicle following distances when sharing the road with human-driven vehicles;
- Develop real-time warnings based on the data derived from the infrastructure support system;
- Optimize the infrastructure support system such as the sensor and V2I facility layout;
- Validate the developed infrastructure support system through simulations and field tests.

In addition, the team will use the results from this development to enhance curricula that would engage and mentor students in the practice of developing safe smart cities. This project will involve three graduate students and several undergraduate students. The trainings through this project will prepare students for potential careers in smart city developments.

17. Key Word Autonomous vehicles, infrastructure sensors, V2I, car-following model		18. Distribution Statement Public distribution	
19. Security Classif. (of this report) Unclassified	20. Security Classif. (of this page) Unclassified	21. No. of Pages 36	22. Price n/a

Form DOT F 1700.7 (8-72)   Reproduction of completed page authorized

Infrastructure Safety Support System for Smart Cities with Autonomous Vehicles

Prepared By

Dr. Ying Huang
Associate Professor
North Dakota State University
Department of Civil and Environmental Engineering
Fargo, North Dakota, 58102
ying.huang@ndsu.edu
Tel: (701) 231-7651
ORCID: 0000-0003-4119-9522

Dr. Pan Lu
Associate Professor/Associate Research Fellow
North Dakota State University
Department of Transportation, Logistics and Finance
Fargo, North Dakota, 58102
pan.lu@ndsu.edu,
Tel: 701-212-3795
ORCID: 0000-0002-1640-3598

Dr. Raj Bridgelall
Assistant Professor/Program Director
North Dakota State University
Department of Transportation, Logistics and Finance
Fargo, North Dakota, 58102
raj.bridgelall@ndsu.edu
Tel: 408-607-3214
ORCID: 0000-0003-3743-6652

Xinyi Yang
Graduate Assistant
North Dakota State University
Department of Civil and Environmental Engineering
Fargo, North Dakota, 58102
xinyi.yang@ndsu.edu
ORCID: 0000-0002-9020-7261

Yihao Ren
Graduate Assistant
North Dakota State University
Department of Transportation, Logistics and Finance
Fargo, North Dakota, 58102
yihao.ren@ndsu.edu
ORCID: 0000-0002-9203-3525

December 2021

Acknowledgements

Disclaimer

The contents of this report reflect the views of the authors, who are responsible for the facts and the accuracy of the information presented. This document is disseminated under the sponsorship of the Department of Transportation, University Transportation Centers Program, in the interest of information exchange. The U.S. Government assumes no liability for the contents or use thereof.

ABSTRACT

A smart city integrates diverse sets of information and communication technologies to monitor asset condition, security, safety, service quality, and operational efficiencies, often in real time. Smart cities are continually hosting a growing number of autonomous vehicles that can sense their environment and navigate without human input. Studies anticipate that autonomous vehicles will significantly improve transport efficiencies, reduce crashes, provide smoother rides, decrease congestion, and simultaneously increase traffic flow through speed harmonization and reduced demand for roadway capacity. The United States Department of Transportation (USDOT) expects that autonomous vehicles could eliminate more than 90% of crashes, depending on their level of adoption (U.S. Secretary of Transportation). Many nations, such United Kingdom, France, Australia, and United States, have welcomed the deployment of autonomous vehicles. As of 2016, seven U.S. states across the nation, together with the District of Columbia, have implemented regulations to involve autonomous vehicle testing and deployment. Despite this momentum and the anticipated benefits, studies show that residents hesitate to embrace autonomous vehicles primarily because of safety concerns. Many expect that the full adoption of autonomous vehicles will take 50 years or longer. Therefore, driverless vehicles will share the roads with human-operated vehicles for a long time. Subsequently, autonomous vehicles of various levels of automation will continue to rely on human inputs. Thus, one of the biggest challenges facing smart cities is achieving fully harmonized vehicle operation in mixed driver scenarios.

This research develops an infrastructure embedded sensor network to provide real-time traffic and road condition information such as traffic volume, traffic composition, vehicle speed, dynamic weight via weigh-in-motion (WIM), traffic density, traffic flow rate, road roughness, and other data to the autonomous vehicles. Accordingly, this study develops a new car-following algorithm that enables autonomous vehicles to integrate the real-time traffic and road condition data from the infrastructure safety support system to support the decision-making processes of autonomous vehicles, such as driving speed and safe vehicle following distances when sharing the road with human-driven vehicles. Micro-simulation results using VISSIM indicated that such an infrastructure safety support system with new car-following algorithm for autonomous vehicles can improve traffic safety and mobility with autonomous vehicles in mixed driver conditions.

EXECUTIVE SUMMARY

This research seeks to develop an infrastructure safety support system by embedding V2I enabled sensor networks into the transportation infrastructure to provide autonomous vehicles and human drivers with inputs to improve their decision making when obvious decisions may not possible. A new car-following algorithm is also developed to enable the autonomous vehicles to integrate the real-time traffic and road condition data from such an infrastructure safety support system to improve traffic safety and mobility with autonomous vehicles in mixed driver environments. The performed sensitivity study also optimizes such an infrastructure safety support system for combined considerations on effectiveness and affordability of the system.

TABLE OF CONTENTS

LIST OF TABLES

LIST OF FIGURES

1. INTRODUCTION

A smart city is operationally defined as one that wisely manages its investments in human and social capital, as well as traditional (transport) and modern (information and communication technologies) capital, to achieve sustainable economic growth and a high quality of life (Caragliu et al. 2011). A smart city is also known as a digital city since it supports digital media (high-tech and creative industries) to share information (Hollands 2008). Incorporating new sensing, communication, and social capacities with vehicles is one of the key aspects of a smart city. The fundamental step to make a smart city is to achieve the goal that autonomous vehicles access data through mobile wireless sensing and communication.

As for the future ground transportation method, autonomous vehicles (AVs) are anticipated to significantly improve transport efficiencies, reduce crashes, provide smoother rides, decrease congestion, and simultaneously increase traffic flow through speed harmonization and reduced demand for roadway capacity (National Highway Traffic Safety Administration 2008; Bierstedt et al. 2014; Leech et al. 2015; Greenblatt 2016; Litman 2017). The USDOT expects that AVs could eliminate more than 90% of crashes (Shanker et al. 2013). However, the effectiveness of AVs on improving congestion and mobility is significantly dependent on their level of adoption, and studies show that residents hesitate to embrace AVs primarily because of safety concerns (National Highway Traffic Safety Administration 2013). The full adoption of AVs will take decades (Committee S.O.-R.A.V.S. 2018). During the long time period before the full adoption of AVs, they will share the roads with human-operated vehicles.

Therefore, it becomes extremely important to develop new technologies to improve the safety and mobility of AVs in mixed traffic conditions. If AVs can be self-aware to make learned and ethical decisions to avoid crashes in multimodal and diverse settings, their safety and mobility in mixed driver environments will significantly improve as well. To become self-aware, in addition to information sensed by on-vehicle sensors and from connected vehicle communication, reliable traffic monitoring technologies monitored from infrastructure sensors on and beside roads may also help AVs extract information that describes vehicle characteristics and their movements on the road (i.e., vehicle velocity, traffic flow, travel time, vehicle density, vehicle dimension, length of traffic jams, etc.). Such an infrastructure traffic monitoring system can collect data that can be applied to the innovative car-following models to improve the safety and mobility of AVs in mixed driver environments.

This project develops such an infrastructure safety support system with on-road sensor networks, which can communicate with AVs through vehicle-to-infrastructure (V2I) to provide AVs and human drivers with inputs to improve their decision making when obvious decisions may not possible. The specific research objectives of this project are to:
   (1) Develop an infrastructure embedded sensor network to provide real-time traffic and road condition information such as traffic volume (e.g., ADT, peak-hour traffic), traffic composition (vehicle classification), vehicle speed, dynamic weight via weigh-in-motion (WIM), traffic density, traffic flow rate, road roughness, and other data;
   (2) Develop algorithms that the infrastructure safety support system will use to process the sensor-based real-time traffic data and pavement conditions to support the decision-making processes of autonomous vehicles such as driving speed and safe vehicle following distances when sharing the road with human-driven vehicles;
   (3) Optimize and validate the developed infrastructure support system through simulations.

In addition, the team will use the results from this development to enhance curricula that would engage and mentor students in the practice of developing safe smart cities. This project will involve three graduate students and several undergraduate students. The trainings through this project will prepare students for potential careers in smart city developments.

Thus, this report is organized according to objectives. In Chapter 2, a brief introduction on the development of the infrastructure sensor network for traffic and road condition monitoring is described; Chapter 3 introduces the development of the new V2I algorithms of the infrastructure supporting system; Chapter 4 illustrates the optimization and the validation of the developed sensor network and V2I algorithm using an autonomous vehicle prototype with a simulated mixed driver environment; Chapter 5 shows the curriculum and educational development of this project, including student mentoring and outreach activities; and Chapter 6 summarizes the conclusions and recommendations from the study.

2. INFRASTRUCTURE SENSOR NETWORK FOR TRAFFIC AND ROAD CONDITION MONITORING

To monitor traffic on roads, visual tracking using roadside cameras is the most commonly applied technology. However, the effectiveness of visual tracking depends significantly on weather conditions, which may limit detection during extremes such as during winter storms when the visibility is limited. In addition, it is challenging for the visual inspection to obtain some important traffic information such as vehicle weight and road roughness. To measure vehicle weights on roads, in addition to other traffic data, several in-pavement sensors that can be considered, including piezoelectric sensor, bending plates, and load cells (Liu et al. 2006). However, these electrical sensors generally show a relatively high cost and short design life, but with moderate accuracy. In addition, these common electrical sensors are highly affected by the surrounding environment (such as moisture). These sensors also have some disadvantages, such as susceptibility to electromagnetic interference (EMI), and extended traffic shut-downs for installing the sensors within the road (Bushman and Pratt 1998; Wierzba and Kosmowski 2000).

In recent years, optic fiber sensors have been used for traffic engineering applications due to their unique advantages: small size, light weight, high sensitivity, immunity to EMI, ability to be embedded in a hostile environment, low cost of less than $1,000, easy installation, and long design life (Mendez 2007; Malla et al. 2008). These advantages may provide a potential solution for reliable long-term in-pavement traffic monitoring sensors. Currently, Fiber Bragg Grating (FBG) sensors are commonly used for civil engineering applications and have been widely accepted in field applications to measure loads, strain, and temperature (Lee 2003; Majumder et al. 2008). A single FBG sensor could potentially provide many, if not all, traffic and road condition data, such as vehicle weight, vehicle speed, vehicle type, pavement fatigue, and temperature. All these advantages can extend the system's durability (Meller et al. 1998). Hence, FBG sensors can be a potential solution for the traffic monitoring system. However, a bare FBG sensor, which is composed of glass material, is very weak without packaging, which is not practical for applications inside pavements with harsh construction processes. Thus, there is an urgent need to develop a robust packaging method for FBG sensors to monitor traffic in a long-term and reliable manner. Glass-fiber-reinforced polymer (GFRP) material, which has become widely accepted for use in civil engineering applications, provides durable and reliable packaging (Oh and Sim 2004). Hence, previous research used the GFRP material to package a three-dimensional (3D) FBG sensor to improve its ruggedness.

In addition, for road condition inspection, various established methods to evaluate the ride quality of a road section and investigate surface irregularities (Loprencipe and Zoccali 2017). Transportation agencies widely use the international roughness index (IRI) to quantify ride quality, which is an indicator of pavement condition. IRI produces longitudinal elevation profiles showing variation in surface roughness by using special inertial profiler vehicles, which require skilled labor to operate and to evaluate the data. Some shortcomings associated with this procedure include the fixed reference speed of 80 kilometers-per-hour required by the golden car model (Bridgelall 2013), a high cost of about $6.12 per mile (McGhee 2004), and wavelength biases due to the fixed quarter-car model used to calculate IRI (Marcondes et al. 1991). The use of smartphones has become a potential alternative approach to measure roadway roughness to reduce cost, increase monitoring frequency, and increase coverage network-wide (Forslöf and Jones 2015). In-pavement sensors also have been used to measure road roughness (Zhang et al. 2015a).

Thus, this study develops an effective in-pavement sensing network based on GFRP-packaged FBG sensors for a robust and cost-effective long-term traffic and road condition monitoring system. Specifically, seven different traffic and road conditions are monitored using the in-pavement sensing network, including: 1) vehicle speed, 2) vehicle wheelbase (Al-Tarawneh and Huang 2018), 3) vehicle weight in motion (WIM) (Al-Tarawneh and Huang 2017; Zhang et al. 2017; Al-Tarawneh et al. 2019;

Zhang et al. 2019, 4) vehicle counting, 5) vehicle classification (Al-Tarawneh et al. 2018), 6) road roughness (Yang et al. 2020; Ahmed et al. 2021), and (7) cracks inside pavements (Alshandah et al. 2019 and 2020). For the detailed developments of these sensing networks please refer to journal and conference publications generated from this project listed after each traffic and road condition parameter. Below is a summary of the sensor network development and the estimation of these data based on the monitoring.

2.1   Infrastructure Traffic Monitoring Sensor Network

An effective infrastructure traffic monitoring system requires a sensor network with multiple sensors inside the pavements for data collections. To ensure the detection of all the needed traffic and road condition data, it requires an accurate vehicle speed estimation. Therefore, a sensor network with an acceptable speed estimation error will be needed to construct an effective traffic monitoring system. Numbers, locations, and distances between sensors are the major factors influencing the accuracy of a sensor network. To effectively estimate vehicle speed, wheelbase, and vehicle classification, requires a minimum of two sensors in the network which need to be installed under the vehicle wheel path for maximum measurement sensitivity. The optimized distance between the two in-pavement sensors in the network for vehicle detection and classification usually falls between 7 ft. and 20 ft. (Bajwa et al. 2011; Udd and Kunz 2003). Also, the variation caused by the inaccurate installation of the sensors (D is the distance between parallel sensors) will cause some systematic error in speed estimation, thus resulting in errors in vehicle classification and other traffic data estimation. To minimize this installation systematic error, the distance between sensors should be large enough to get maximum speed estimation accuracy (Doi 2004). In this study, a sensor network is formed using the minimum numbers of sensors required, which is two 3D GFRP-FBG sensors previously developed by the PI's research group, as shown in Figure 2.1 on the left side for the detailed dimensions of the used sensor. As shown in Figure 2.1, a distance of 16 ft. between the two sensors is used, which is between 7 ft. and 20 ft. as suggested by the literature. The sensors are installed under the wheel path to be more accurate for vehicle passing measurements. In addition to the two 3D GFRP-FBG sensors, to eliminate the temperature effects, one temperature compensation FBG sensor was installed 2.42 ft. away from the 3D-2 sensor to monitor the pavement temperature variances. Also, to study the multiple tire and dynamic effects, a 1D GFRP-FBG sensor was installed on the side of Sensor 3D-2 as shown in Figure 2.1 (Al-Tarawneh and Huang 2018).
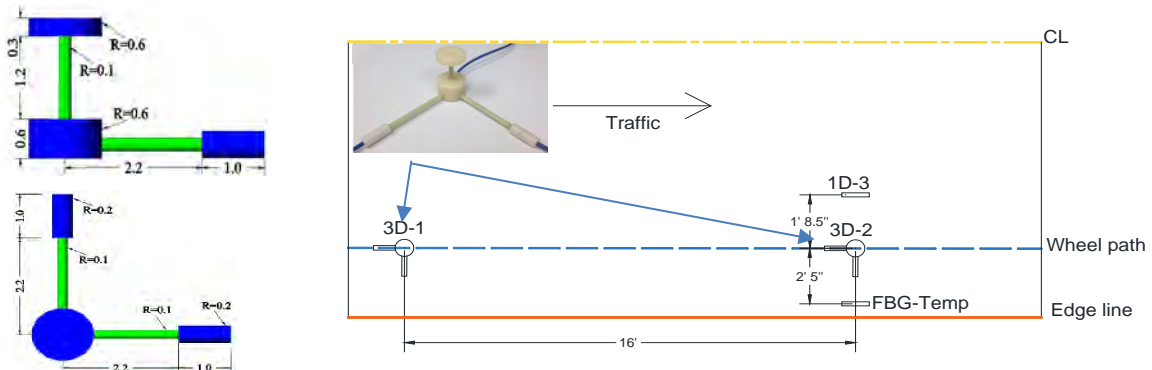
Figure 2.1 3D GFRP-FBG sensor and the infrastructure sensor networking
(3D: three dimensions, 1D: one dimension, CL: center line)

To validate the developed traffic monitoring system as shown in Figure 2.1, field testing was performed at the Cold Weather Road Research Facility in Minnesota (MnROAD) of the Minnesota Department of Transportation (MnDOT). MnROAD consists of two unique roadways: a two-lane low-volume loop that is loaded with a 5-axle 40-ton (80 kips) semi-truck and a section of interstate I-94 "mainline" that contains two westbound lanes with live traffic. The developed sensor network in Figure 2.1 was installed inside Pavement Cell 17, one section of I-94 at MnROAD, which belongs to the I-94 mainline westbound

4

lanes as shown in Figure 2.2 (a). The 3D GFRP-FBG sensors were installed beneath the wheel path on the asphalt pavement as shown in Figure 2.2 (b). The longitudinal components of the 3D sensors were installed at the bottom of the road asphalt layer (5 in. under the road surface) and the vertical components of 3D sensors were installed in the base layer and sealed with asphalt sealing to fix it in the desired location (1.6 in. beneath the base layer) and to reduce the failure risk due to compaction during the paving process. After the installation of the sensor network, the three components of the sensors in the network together with a temperature compensation FBG sensor were connected to an FBG integrator with a 5 KHz sampling rate (which is efficient for WIM measurement at low and high speed when the sampling rate more than 1.2k (Zhang et al. 2015b)). The FBG integrator was further connected to a personal computer to record the data.

Figure 2.2 (a) MnROAD facility and (b) the sensor installation scene

2.2   Vehicle Speed and Wheelbase Detection

When a vehicle tire passes over the road, the pavement produces strain signals and the strain changes on an FBG sensor will produce corresponding Bragg wavelength changes, which can be recorded and analyzed to recover the strain information inside the pavements as shown in Figure 2.3. To derive the wheelbase of a vehicle, it is very important to accurately estimate the vehicle speed. Because the distance between the two sensors in the sensor network, 3D-1 and 3D-2, is a known parameter (D) which was selected to be 4.88 m (16 ft.) in this study (as seen in Figure 2.1), with the recorded time, the vehicle driving speed can then be estimated by dividing D over t where t is the time interval between the peaks of the two sensors for the same axle of a vehicle. Because there is a minimum of two axles for a vehicle, the time intervals can be measured twice by using the first peaks of the two sensors in the network (t1) and the second peaks of the two sensors (t2) as shown in Figure 2.3. Thus, the accuracy of speed estimation can be improved by taking the average of the two adjective sensor peaks. Therefore, by knowing the vehicle driving speed (v), the vehicle's wheelbase can be estimated as v times t. Also, the accuracy of wheelbase estimation can be improved by taking the time estimation average of the two adjective sensor peaks.

A 5-axle semi-truck with total gross weight of 80 kips (36.29 tons) was used to validate the developed system for speed and wheelbase detection. The truck moves on top of the sensor at different high speeds (25, 35, and 45 mph). Figure 2.4 shows the axle load distribution of the truck at each axle. The truck has estimates for the wheelbase distances of 17.042, 4.542, 33.75, and 4.167 feet, respectively.
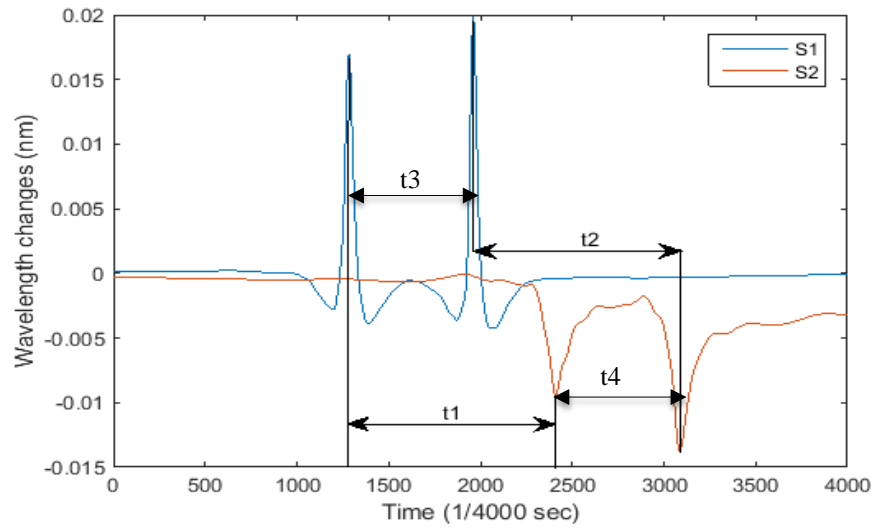
Figure 2.3 Sensor responses for a passing two-axle vehicle

Figure 2.4 MnROAD loading truck.

The speed measurement results from the vehicle classification system were compared with the results from a radar gun to validate the system measurement accuracy. Table 2.1 shows the comparison of the speeds and wheelbase measurements between the estimated values from the developed system and that from the reference calculated from a radar gun. From Table 2.1, the system can estimate the speed and the wheelbase with an accuracy of 95% or higher.

Table 2.1 Speed and wheelbase measurements for 5-axle truck

Number	V (ft/sec)	Actual V (ft/sec)	V-error (%)	WB (ft)	Actual WB (ft)	WB-error (%)
1	36.89	36.667	0.61	16.953	17.042	0.52
2	36.89	36.667	0.61	4.744	4.542	4.45
3	36.89	36.667	0.61	33.806	33.75	0.17
4	36.89	36.667	0.61	4.268	4.167	2.42
5	51.912	51.333	1.13	17.048	17.042	0.04
6	51.912	51.333	1.13	4.719	4.542	3.90
7	51.912	51.333	1.13	33.629	33.75	0.36
8	51.912	51.333	1.13	4.192	4.167	0.60
9	62.943	61.6	2.18	17.202	17.042	0.94
10	62.943	61.6	2.18	4.721	4.542	3.94
11	62.943	61.6	2.18	33.609	33.75	0.42
12	62.943	61.6	2.18	4.183	4.167	0.38

2.3   WIM Measurements

In this research, the multilayer system theory is used to determine stress and strain through the flexible pavement to measure the weigh-in-motion (WIM) of passing vehicles. The 3D GFRP-FBG sensor is embedded inside a flexible pavement with six layers. Each layer has three parameters: modulus of elasticity E, Poisson's ratio v, and depth. By applying the classical theory of elasticity and considering that x-direction is the longitudinal direction of the 3D GFRP-FBG sensor, which is parallel to the wheel path, y-direction is the transverse direction of the sensor, which is perpendicular to the wheel path, and z-direction is the vertical direction of the sensor, which is beneath the asphalt surface, the strain components under the circular loaded area in the three directions can be found (Huang 1993). Because a multi-layer system poses difficulties for analyzing flexible pavement theoretically, the KENLAYER software established by Huang (1993) is used in this study to determine the strains at the sensor location and to perform sensitivity a study. KENLAYER can be applied to determine stress, strain, and deflection at any point in the layered systems under single, dual, dual-tandem, or dual-tridem wheels with each layer behaving differently. To get the weight sensitivity functions of the GFRP-FBG sensor for the three components, the strain at the locations of the three components are calculated for one-unit load using KENLAYER software and represented longitudinal, transverse, and vertical components, respectively. After the estimation of strain sensitivity of each sensor component (A_L, A_T, and A_v), WIM measurement (wheel load, P) in three directions (longitudinal, transverse, and vertical direction) can be computed based on the measured center wavelength changes from the FBG sensors as:

$$P = A_L\left(\frac{\Delta\lambda_L}{\lambda_L} - \frac{\Delta\lambda_{Te}}{\lambda_{Te}}\right) = A_T\left(\frac{\Delta\lambda_{Tr}}{\lambda_{Tr}} - \frac{\Delta\lambda_{Te}}{\lambda_{Te}}\right) = A_V\left(\frac{\Delta\lambda_V}{\lambda_V} - \frac{\Delta\lambda_{Te}}{\lambda_{Te}}\right) \tag{1}$$

in which λ_L, λ_{Tr}, λ_V, and λ_{Te} are the measured center wavelengths from longitudinal, transverse, and vertical components of the 3D GFRP-FBG sensor and the temperature compensation sensor, respectively.

The sensitivity of the 3D GFRP-FBG sensor for WIM measurement in all three dimensions (A_L, A_T, and A_v) are significantly influenced by different factors, such as sensor installation depth, host material property, and the location of the wheel path. The longitudinal and transverse components of the 3D sensor show highest measurement sensitivity either on the surface of the pavement or on the bottom of the asphalt layer, and the vertical component has the highest sensitivity near the middle of the HMA layer. If

7

installed on the surface of the pavement, the sensor will be vulnerable to damage, resulting in a shorter service life. Thus, the recommended practice is to install the sensor at the bottom of the asphalt concrete layer to secure the best measurement sensitivity. For the highest measurement accuracy, the future WIM measurements will use the measurements from the longitudinal components of the 3D sensors.

Table 2.2 compares the WIM measurements from the longitudinal component of the 3D sensor with the reference weights for each truck axle at 5 mph and 45 mph vehicle speeds. When compared with the reference weights, which are the actual truck's weights at each of the tires, the longitudinal component of the sensor has a measurement error of 13.2% and 10.5% at 5 mph and 45 mph, respectively. Errors for Axle 1 are larger than for the other axles because its weight is less than other axles. Consider the following situations: 1) There are only three sensors, and the position of the sensors cannot be changed according to the moving vehicles; 2) Based on the infrastructure sensor network shown in Figure 2.1, when the vehicles pass through, only one or two sensors can measure the wheels' weight; 3) The wheels cannot be placed exactly in the front of the sensors. This study assumes that the weight is equally distributed on each wheel to estimate the weight of the vehicle. The measurement errors of Axle 4 are higher than Axle 2,4, and 5, which are able to decrease by adding sensors. This study serves as a preliminary study to investigate the feasibility of the GFRP-FBG sensor for WIM systems in flexible pavement. As seen in Table 2.2, there is a large variance of measurement error between different axles. The major contributor to this variance of error which may be the variance of loading position for each axle. Because the 3D sensor is still categorized as a point sensor and the loading position for each axle is not the same when the vehicle is passing the sensor location, this error may be significant.

Table 2.2 Comparison of the WIM measurements with references

Measured Weight	Axle 1		Axle 2		Axle 3		Axle 4		Axle 5	
	WIM (Kips)	Error (%)	WIM (Kips)	Error (%)	WIM (Kips)	Error (%)	WIM (Kips)	Error (%)	WIM (Kips)	Error (%)
Reference	5.8	-	9.05	-	8.05	-	8.6	-	8.2	-
5 mph	4.5	21.9	8.15	9.9	7.31	9.14	6.98	18.82	7.4	9.34
45 mph	4.37	14.32	8.82	1.9	8.28	4.49	6.94	17.8	7.27	12.7

2.4   Vehicle Counting and Classification

In 1980, the Federal Highway Administration (FHWA) developed a vehicle classification system (Hallenbeck et al. 2014), that divided vehicle types depending on the number of axles and the wheelbase (Hallenbeck et al. 2014). However, establishing a fixed threshold for classifying a vehicle is difficult. Many effective pattern recognition methods have been used for vehicle classifications in the literature, including a vision-based preceding vehicle recognition method (Kato et al. 2002), inductive classifying artificial network (ICAN) (Sun et al. 2003), fuzzy inference system (Sroka 2004; Nelson 2001), the probabilistic neural network method (Selekwa et al. 2005; Mussa et al. 2006), and the support vector machines (SVM) learning method (Scholkopf et al. 1997). The SVM machine learning classifier predicts the output from the given input and is reported as a well-founded technique in statistical learning theory (Scholkopf et al. 1997). In this research, a vehicle classification system was developed based on a sensor network from GFRP packaged FBG sensors supported by the SVM machine learning method, neural network (NN), and k-nearest neighbors (KNN) algorithms to extract the vehicle classification information.

FHWA (Hallenbeck et al. 2014) divided vehicles into 13 categories based on the number of axles and the wheelbase. According to the FHMA standard, vehicles are divided into six classes: passenger cars, motorcycles, buses, other 2-axle 4-tire vehicles, single-unit 2-axle 6 tire or more trucks, and combination trucks. Taking into account the limited numbers and types of vehicles collected, and all classification

validation are based on the videos which not clearly enough to clearly identify the difference between these 13 types of vehicles. In this research, vehicles are sorted into three categories depending on the flow type in the selected case study as shown in Table 2.3. Because the multiple data sources can give a more efficient performance and yield higher accuracy, a centralized fusion strategy was used in this paper, as shown in Figure 2.5. This strategy collects parameters from data sources and combines them to form one input dataset; then a multiclass SVM is trained to decide on vehicle classes.

Table 2.3 Vehicle class description

Vehicle type	Class	Number of axles	Axles distribution	FHWA category
Small vehicles	C1	2	1F+1R	Passenger car, 2-axle 4-tire vehicle
Medium-large trucks	C2	2	1F+1R	2-axle 4-tire vehicle, 2-axle 6-tire trucks
Single unit trucks- combination of trucks	C3	3-6	1F+2R 1F+2M+2R 1F+2M+3R 1F+1M+1R 1F+1M+2R	single-unit 2-axle 6-tire trucks, trucks combination
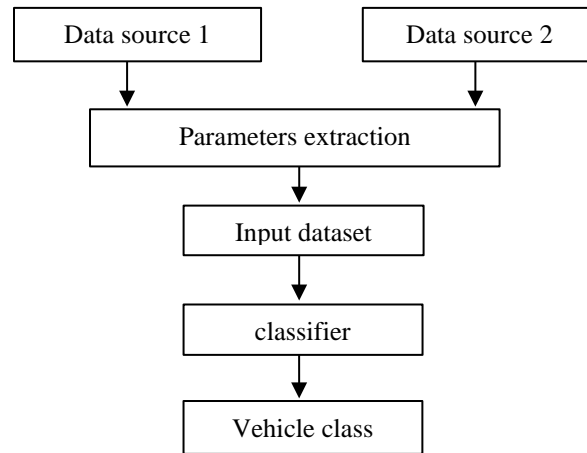
Figure 2.5 Data fusion strategy scheme

To validate the vehicle counting and classification capability, one longitudinal component of sensor 3D-1 (S1) and one vertical component of sensor 3D-2 (S2) in the sensor network, as shown in Figure 2.1, were used to feed the vehicle classifier for classification. Two hours of real-time traffic data were collected. During the two-hour period, a total of 477 vehicles were recorded. The recorded dataset for each vehicle type (C1, C2, and C3) were divided into a training set (50% of the data) with 241 vehicles, a validation set (25% of the data) with 117 vehicles, and a test set (25% of the data) with 117 vehicles of randomly selected records. Table 2.4 shows the detailed number of vehicles in each class for all three datasets and Figure 2.6 shows a two-minute data example from one of the infrastructure sensors.

Table 2.4 Collected real-time vehicle classification data

Class	Training set	Validation set	Test set
C1	133	65	65
C2	22	11	11
C3	86	42	42
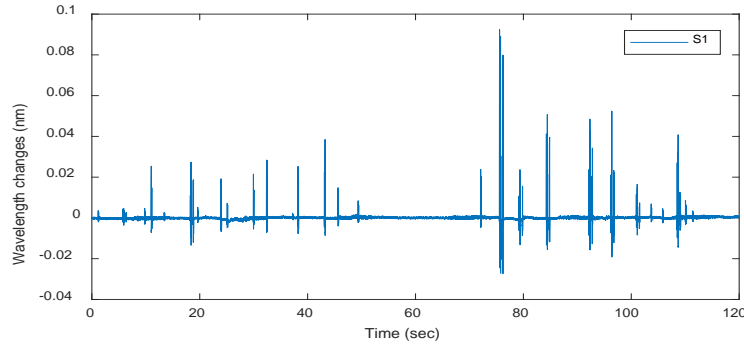
Figure 2.6 S1 sensor's response for 2 minutes real traffic

To classify a vehicle into the three categories above, two SVM methods, including the one-against-all (OAA) and the one-against-one (OAO) methods (Chen et al. 2009), and the NN, and KNN methods, can be considered. To solve the vehicle classification problem, the MATLAB Classification toolbox was used in this paper for multi-class classification problems. The accuracy of different classifiers is shown in Table 2.5. Both the OAO and OAA algorithms work well for the developed system to classify vehicles with real traffic. The OAO method (>94% accuracy) has slightly higher accuracy than the OAA method (>90% accuracy). When SVM methods were compared with KNN and NN methods, the results from SVM-OAA and NN have slightly higher accuracy than KNN and SVM-OAO. The difference between algorithm performances for vehicle classification is not significantly clear; it may be because of the small dataset used in this research.

Table 2.5 Classification accuracy with OAA, OAO, NN, KNN methods

	C1	C2	C3
OAA	99%	94%	100%
OAO	99%	91%	100%
NN	99%	94%	100%
KNN	98.5%	90%	100%

2.5 Road Condition Detection

The roughness of roads was measured using both in-pavement sensors and smartphones on vehicles to quantify the road conditions. Previous studies showed that the developed infrastructure sensor system can also detect road roughness. Based on the strains detected from the 3D GFRP-FBG sensors, the roughness of the roads can be estimated (Zhang et al, 2015a). The international roughness index (IRI) is one of the most frequently used characterizations of road roughness or ride quality. However, use of the IRI requires trained staff to operate specialized equipment driving at a fixed speed, resulting in a relatively high cost. Therefore, both infrastructure sensors and smartphones used the ensemble average RIF (EAR) index, based on the road impact factor (RIF) transform, to describe road roughness. Previous research already established a relationship between the EAR index and the commonly used IRI index (as shown in Table 2.6) using three different panels, which can be used to measure the road conditions for testing Cell 17 at the MnROAD facility.

Table 2.6 Comparison of IRI and EAR-index on sensor-deployed panels (Zhang et al. 2015a).

	Panel 36	Panel 40	Panel 53
IRI derived from strain-based method	3.33	3.34	3.19
EAR index from the connected-vehicle method	0.149	0.162	0.144
IRI/EAR index	22.35	20.62	22.15

In addition to the roughness, the cracks inside pavements can also be monitored using the infrastructure FBG sensors. To validate this capacity, FBG sensors were embedded into three sample pavements and cracks were detected using the FBG sensors and visual inspection as shown in Figure 2.7. Algorithms were developed to detect the crack locations (Alshandah et al. 2020). Table 2.7 summarizes the comparison of maximum variance of crack location calculated from developed analytic analysis and measured from experimental results from all three samples which tested for compression, tensile, and flexural strength tests. Table 2.7, indicates that the average variance between the crack pattern detected using the discrete sensors on the bottom of the concrete beam and the actual crack pattern for all three samples is 17.6 %, indicating a very promising crack detection approach for field internal crack detection. The maximum error of 30.1% was shown in Sample 2 because the crack location was very close to the sensor location and induced some potential damage to the sensor. However, for the other samples where the cracks were not generated directly on the sensors, the detection accuracy was below 17.7% as indicated from the experiments.
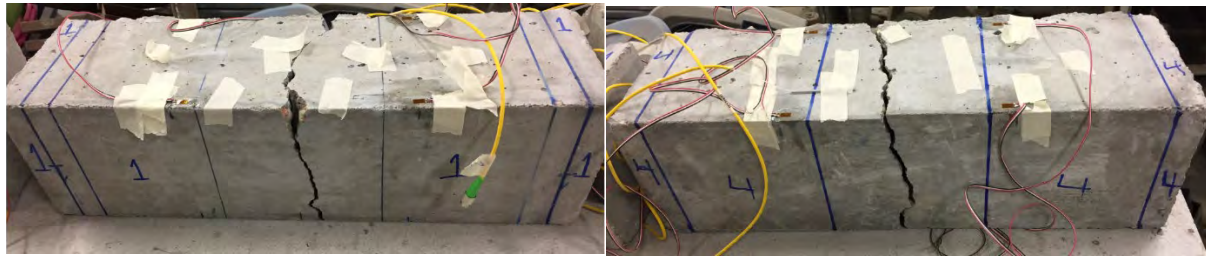
Figure 2.7 Example sample 1 and 2 for in-pavement crack detection using strain sensors

Table 2.7 Comparison of maximum variance of crack location calculated from developed analytic analysis and measured from experimental results

Sample Number	Analytical solution calculated from developed sensing plan (mm)	Experimental result measured from the experiments (mm)	Maximum error (%)
Sample 1	106	114	5
Sample 2	146	100	30.1
Sample 3	120	135	17.7
Average			17.6

3. DEVELOPMENT OF THE NEW V2I ALGORITHM OF THE INFRASTRUCTURE SUPPORTING SYSTEM

To drive automatically, an AV relies on sensors on board the vehicle, such as video cameras, radar sensors, ultrasonic sensors, lidar, global positioning systems, and the central computer (Younsi et al. 2020; Harlow and Peng 2001; Wu et al. 2020; Tang et al. 2020). The cameras, radar sensors, and lidar units are used to detect surrounding information, such as the distance to objects (e.g., pedestrians) and traffic signs, as well as speed and acceleration of nearby objects. The autonomous vehicles will then send all that information to the central computer. The computer combines and organizes the data collected by the ego autonomous vehicles and communication with other devices to control the autonomous vehicles' behavior. Any autonomous vehicle requires a car-following model to be functional when the robot car is driving by itself on a road. A car-following model, as a basic model used in traffic flow simulation, can simulate the behaviors of vehicles, and provide recommendations of AV reactions.

3.1 Current Status of Car-Following Algorithm for AVs

There are many kinds of car-following models, such as stimulus-response models, safe-distance models, desired headway models, psychophysical models, and artificial intelligence models (Chen et al. 2016; Brackstone et al. 1999; Aghabayk et al. 2015). Among those, the stimulus-response model is a widely used car-following model. It assumes that each driver responds to the stimulus from the other vehicles. The stimulus includes parameters such as velocity, acceleration, and headway. The three most commonly used stimulus-response car-following models were reviewed with the advantages and challenges, including the cooperative adaptive cruise control (CACC) and adaptive cruise control (ACC) models, the optimal velocity model (OVM), and the multi-anticipative car-following model.

Adaptive cruise control (ACC) extends the traditional cruise control (CC) system, which reaches and maintains the vehicle's preset speed (Stanton and Young 2005). As the first driver control assistance system entering the market, ACC has the potential to influence traffic flow characteristics (VanderWerf et al. 2001). ACC systems can automatically adjust speed based on the desired spacing or speed from the preceding vehicle. CACC has better performance on collision avoidance and safety than ACC since it not only receives the information from preceding vehicles but also the vehicles ahead of the preceding one (Milanés et al. 2013). The CACC/ACC model well represented the behaviors of the vehicles. However, it controls the behavior of the model based only on the information of the target vehicle, even though the following vehicle can get information from multiple vehicles ahead of it. In addition, the vehicle with the CACC system can only communicate with other autonomous vehicles equipped with the CACC systems. Therefore, CACC systems can work well if autonomous vehicles are fully adopted. Unfortunately, the full penetration of autonomous vehicles into the road network will take decades, during a time when human drivers will share the same road systems with autonomous vehicles. In such a mixed driver condition, most accidents associated with autonomous vehicles are induced by the operational inconsistency of human drivers.

To better use the information obtained from multiple vehicles before the ego vehicle, the OVM (only related to the preceding vehicle) and multiple-anticipate car-following model (using the information from multiple preceding vehicles) can be considered. The OVM, first developed by Bando et al. (Bando et al. 1995), is a well-known car-following model and considered a prominent stimulus-response model. The OVM performs based on four assumptions (Bando et al. 1995): 1) the motion of each vehicle is based on the responses of the driver to the stimulus from other vehicles; 2) the driver can express the response by acceleration, which is direct control by the driver; 3) each vehicle has a legal velocity, which depends on the headway of the preceding vehicle; and 4) there is no time lag of response. Based on these assumptions, the OVM sets the stimulus as the difference between the optimal velocity and the velocity of

the considered vehicle, and the sensitivity is a constant factor. However, sometimes the OVM showed extremely high acceleration because the empirical accelerations were limited to constant.

The unrealistically high acceleration and deceleration of the OVM can be resolved by using the multi-anticipative car-following model, which was developed by Lenz (Lenz et al. 1999). The multi-anticipative car-following model solves the problem of instability in the dynamical behavior of the OVM model by considering the reaction to more than one vehicle ahead of the ego vehicle. Although the multi-anticipating model considered the stabilization of dynamical behavior by multiple preceding vehicles, the desired velocity depends on the average clearance of preceding vehicles, which will influence the accuracy of the result when vehicles operate at non-normal velocity and accelerations. In addition, the desired velocity in the traditional multi-anticipative car-following model depends on the average car following clearance of the vehicles in front of the AVs, which might lead to errors because it ignores the influences of any unusual conditions such as car crashes.

3.2   The New Cumulative-anticipative Car-Following Algorithm

Vehicle-to-everything (V2X) communication can solve the operational inconsistency between human drivers and autonomous vehicles because it passes information between the vehicles and other devices that may affect driving to avoid collisions, reduce traffic congestion, and improve the driving environment. The V2X communication is an integration of several more specific vehicular communication systems (Chen et al. 2017), including vehicle-to-vehicle (V2V) (Harding et al. 2014; Gupta et al. 2020), vehicle-to-pedestrian (V2P) (Craig et al. 2017), vehicle-to-network (V2N) (Kim and Kwak 2016; Sun et al. 2016), and vehicle-to-infrastructure (V2I) (Milanes et al. 2012). Autonomous vehicles can significantly reduce human errors by collecting numerous data and information that can be used in autonomous driving models.

Based on the various monitored traffic and road condition data from the infrastructure sensor network described in Section 2, a new V2I algorithm car following model is needed and is developed in this research as the cumulative-anticipative car-following (CACF) model, which provides these traffic and road conditions to the AVs with enhanced decision-making capacity. Different from the traditional multi-anticipative car-following model, the new CACF model developed in this project uses the actual measured information of vehicles from V2X systems to calculate the desired velocity and acceleration of the AVs. The CACF model can then predict the driving distances after every system time period with the actual measured traffic data and the desired data separately and also calculate the difference between them. Instead of simply summing all the differences of predicted desired clearance and predicted clearance of each vehicle together and dividing the sum by the total number of vehicles, the new CACF model considers the influences of every two adjacent vehicles' interaction. The new CACF model applies the difference of predicted desired clearance and predicted clearance to provide assistance to the following vehicles one by one and guide the AVs to safer decisions. In addition, the new model also considers the crashes and set factors to avoid the influences of crashes.

Specifically, in the new CACF model, reference preceding vehicles will need to be selected as shown in Figure 3.1. Not all the vehicles ahead of the ego vehicle will be considered as reference vehicles. Based on the headway between each of the two preceding vehicles, the CACF model will only select the vehicles (in green) whose headway is less than the maximum range of the vehicles' headway (h) (Considering the RADAR-equipped vehicles are not able to collect the information about vehicles that fall beyond 50 meters (Brogg et al. 2008, Park et al. 2016)) and ignore other vehicles (yellow). The value of the maximum range of the vehicles' headway (h) depends on the speeds of vehicles and the volumes of the road.
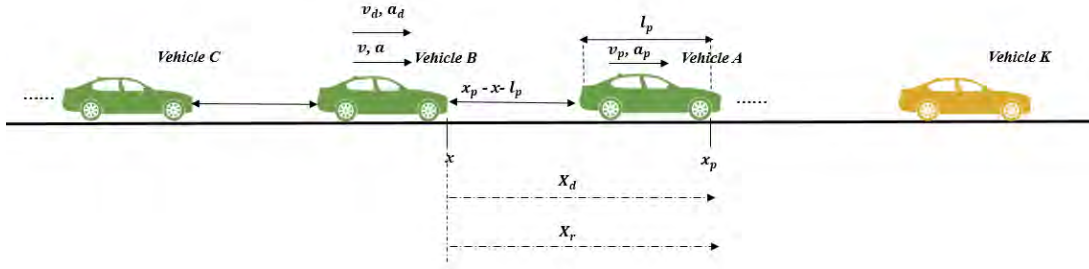
Figure 3.1 Schematic of the new CACC model

After each reference preceding vehicle is selected, the desired velocity of the next vehicle (v_d) can be calculated based on the coordinate of itself and the vehicles before it (x and x_p), the length of the preceding vehicle (l_p), actual velocity of itself and the vehicles before it (v and v_p), actual acceleration of the following vehicle (a) and predicted clearance of desired and real data of the preceding vehicle (X_d and X_r), as below:

$$v_d = g * \left[v_p + k_d * (r - t_{system} * v)\right] + m * \{v_p + k_d * \left[r - t_{system} * v + (-1)^c * (X_d - X_r)\right]\} + k *$$

$$\left[v + (a * t_{system})\right] \tag{2}$$

in which, g equals 1 if the desired acceleration of the target vehicle is unknown and 0 otherwise; m equals 1 if the desired acceleration of the target vehicle is known and $a_c = a_d$, and 0 otherwise; k is equal to 1 if the desired acceleration of the target vehicle is known and $a_c \neq a_d$, and 0 otherwise; k_d is constant factor; t_{system} is system time period, if the preceding and following vehicles are in the CACC model, the system time period is 0.5s, otherwise, it is 1.4s. c is equal to 1 if $X_d > X_r, r >$ safe distance, and 0 otherwise.

The control acceleration of the following vehicle can then be computed based on the clearance of the following vehicle (r), actual velocity of itself and the vehicles before it (v and x_p), actual acceleration of the preceding vehicle (a_p), and predicted clearance of desired and real data of the preceding vehicle (X_d and X_r), as below:

$$a_c = k_a * a_p + k_v * (v_p - v) + k_d * (r - t_{system} * v + (-1)^c * (X_d - X_r)) \tag{3}$$

where, k_a, k_v is a constant factor. k_a equals 1.0, k_v and k_d equal to 3.0 and 0.2 in accordance with Simulation of Intelligent Cruise control studies and set to 0.58 and 0.1 in the recent study (Van Arem et al. 1997, VanderWerf et al. 2002, Van Arem et al. 2006). Thus, the clearance of the following vehicle at the next system time period can be predicted using the actual velocity and acceleration through the kinematic equation as below:

$$X_r = v * t_{system} + \frac{1}{2} a * t_{system}^2 \tag{4}$$

If the predicted clearance (X_r) is smaller than the predicted desired clearance, it means that the following vehicle maintains more distance from the vehicle ahead of it while it maintains the same velocity and acceleration at the next system time period. Then the difference between the predicted desired clearance and predicted clearance needs to be subjected to the CACF model to decrease the acceleration of the third reference preceding vehicle to increase its headway. However, if the desired distance is less than the predicted clearance, that indicates the following vehicle does not have enough distance from the vehicle ahead of it while it maintains the same velocity and acceleration at the next system time period.

4.   OPTIMIZATION AND VALIDATION OF THE DEVELOPED V2I ALGORITHM

Any data transferred through V2X can be used as inputs to the developed new CACC model in Section 3. However, based on the collected traffic and road condition data from Section 2, a V2I communication was investigated in this research to demonstrate, optimize, and validate the effectiveness of the developed new CACF model. The V2I allows sensors in or alongside traffic infrastructures, such as in-pavement sensors, overhead RFID readers, streetlights, traffic lights, cameras, lane markers, parking meters, etc., to communicate with the AVs,. V2I communication can transfer the traffic and road condition data (such as vehicle location, velocity and acceleration, road roughness) from the infrastructure sensing network to the AVs. The data from the sensing network, which are expected to be accurate and quick, can then be used by the AVs to support their decision making.

4.1   Validation of the CACF Model in VISSIM

To optimize and validate the developed new CACF model, microsimulation using VISSIM was conducted in this research. The VISSIM software is a behavior-based micro-simulation traffic software widely used in urban and highway simulation. The technical features of pedestrians, bicyclists, motorcycles, cars, trucks, buses, trams, and light (LRT) and heavy rail are included in VISSIM to analyze and optimize traffic flow under a variety of traffic conditions, such as lane setting, traffic composition, traffic signals, and bus stops (Fellendorf et al. 2010). The VISSIM-APIs (application programming interfaces) are an add-on module that allows the user to integrate external applications into VISSIM (PTV 2020) and thus enhance the user's experience. It includes COM-Interface, DriverlModel-DLL, DrivingSimulator-DLL, EmissionModel-DLL, and SignalControl-DLL (PTV 2020). The advanced V2I communication features of the AVs are modeled through VISSIM APIs by various researchers (Zhao and Sun 2013; Fyfe 2016; Sukennik and Group 2018; Papadoulis et al. 2019). To evaluate the effectiveness of a new model, the Federal Highway Administration (FHWA) suggests the Surrogate Safety Assessment Model (SSAM), which can analyze vehicle safety in the microscopic traffic simulation model (Huang et al. 2013; Abou-Senna et al. 2015). In this study, SSAM is applied to evaluate the number of conflicts between vehicles to test the suitability of the transportation model. The traffic events could be considered as traffic conflicts when the drivers need evasive maneuvers such as slowing down quickly, changing lanes suddenly to avoid collision (Fyfe 2016). The simulation results could be used to improve the traffic state to reduce congestion and emissions.

To evaluate the effectiveness of the new CACF model, simulation results from the four different models, including the Wiedemann 99, the ACC, the CACC, and the newly developed CACF, were compared using safety and mobility measures. Table 4.1 shows the percentage of reduction in average number of conflicts compared with the new CACF model for the three currently available models. It can be seen that an average of 80% reduction in conflict was noticed for all five speed limits tested.

Table 4.1 Percentage of reduction in the average number of conflicts comparing the new CACF model with other three models at five different speed limits

Speed limit		Wiedemann99	ACC	CACC
55	Average	77.69%	79.31%	83.31%
60	Average	80.20%	84.07%	82.16%
65	Average	83.99%	86.85%	89.60%
70	Average	80.37%	83.33%	83.84%
75	Average	80.93%	87.03%	89.20%

Table 4.2 compares the average velocity of all the vehicles with the four different car-following models at speed limits of 55, 60, 65, 70, and 75 mph, respectively. Compared with the other three models, the new CACF model yielded the highest average speeds between 49.78 mph and 59.80 mph. The velocity of the AVs varied from 46.34 to 54.30, 42.68 to 56.62, 40.26 to 61.36, 37.10 to 53.80, and 37.03 to 58.42 mph at the five different speed limits. In addition, the CACF showed the lowest range and sample variance among the models, indicating that the new CACF model can maintain a more stable driving speed and provide better mobility of AVs.

Table 4.2 Comparison of the mean speeds of the AVs using the four different models at speed limits of 55 mph, 60 mph, 65 mph, 70 mph, and 75 mph

Speed		Wiedemann 99 (mph)	ACC (mph)	CACC (mph)	CACF (mph)
55 mph	Mean	50.77	50.13	49.47	53.56
	Range	2.22	5.58	6.62	1.62
	Standard Deviation	1.14	2.60	3.01	0.73
60 mph	Mean	51.55	49.96	50.83	55.59
	Range	6.18	12.39	8.27	2.00
	Standard Deviation	3.12	5.64	3.75	1.14
65 mph	Mean	53.14	50.52	50.24	59.80
	Range	9.54	17.92	16.72	2.54
	Standard Deviation	4.85	8.17	8.62	1.61
70 mph	Mean	44.50	42.68	43.55	52.07
	Range	9.33	11.66	11.93	4.02
	Standard Deviation	5.39	6.26	6.82	1.88
75 mph	Mean	49.12	44.54	44.29	56.67
	Range	6.63	10.90	13.84	3.44
	Standard Deviation	3.82	6.40	7.89	2.25

Table 4.3 further compares the mobility and safety improvements of CACF with Wiedemann 19 and CACC models, such as capacity, traffic delay, and network safety at varying market penetration rates of 0%, 20%, 40%, 60%, 80%, and 100%. As shown in the first and second rows of Table 4.3, the CACF model increases the overall road capacity by 35% for a 90% market penetration. The average travel time starts to improve from 10% market penetration and is improved by 6.6% for CACC and 9.1% for the CACF model at a 90% market penetration rate. Finally, the average delay is drastically reduced to "0 sec" for CACF at 80% penetration and 0.6 sec for CACC at 90% penetration, respectively. This test shows that the efficiency of mobility parameters is enhanced for both car-following logics. The mobility performance of the CACC and CACF models have low-significance behavior. The CACF model has slight mobility improvements over the CACC model for increasing market penetration rates.

The performance of the CACC and CACF models varies significantly through the course of different market penetration rates as shown in the third row of Table 4.3. More importantly, the safety performance is improved significantly for the CACF model as it proceeds with the penetration rates, unlike the CACC model where the safety analysis has resulted in poor performance for the increasing rate of penetration. It is also noticed that the CACF model maintains a larger gap as compared with the CACC model for mild shockwaves, leading to fewer conflicts. For the TTC value of $\leqslant 3.0$ sec, the number of conflicts is reduced by 64.5% for a 90% market penetration rate using the CACF model.

Table 4.3 Comparison of mobility and safety parameters using the three different models (Wiedemann 99, CACC, and CACF)

Investigating parameters	Mobility	Safety
Maximum CACF Throughput	The road capacity for the CACF model increases by 35% for a 90% market penetration as compared to the VISSIM default Wiedemann 99 car-following model.	-
Mobility performance of CACC and CACF models	The average delay of the Wiedemann 99 model is 13.9 sec. However, the delay is drastically reduced to 0.2 sec and 1.6 sec for CACF and CACF models at 80% market penetration rate, respectively.	
Mobility and safety performance of CACC and CACF models	The mobility performance of both models has low significance.	The CACC model only performs better at 10% market penetration rate. The CACF model drastically improves network safety for increasing market penetration rates.

4.2   Optimization of the Sensor Network

To optimize the sensor network for further system improvements, microsimulation using VISSIM was further applied to perform parametric study of the system of the newly developed CACF model. The sensitivity of the VISSIM default driving behavior using Wiedemann 99 model was analyzed as a reference for comparison. There are three parameters investigated for system optimization, including the V2I communication range, the communication signal response delay, and multi-lane influence, with different penetration rates of 10%, 30%, 50%, and 70%. Table 4.4 shows the summary of results for the optimization results.

As shown in Table 4.4, the communication ranges, such as from 200 to 250 meters, generate minimal average rear-end conflicts for lower and higher market penetration rates. However, the communication range with 150 meters showed a slight increase in conflicts for a 10% to 30% market penetration rate. The higher communication range, i.e., 400 meters, showed somewhat equal results with the base case of 300 meters. The results indicated that the CACF model has low significance for operation range greater than 300 meters. Thus, a communication range from 200 to 250 meters is suitable for the CACF model for a single-lane network. For the capability of communicating with 'n' number of cars, such as five cars ahead, 10 cars ahead, and 15 cars ahead, shows no significance for safety and mobility results. Even if the CACF car communicates with five vehicles ahead, it will maintain a safe behavior because of the nature of the proposed model implementation. Hence, it indicates that the CACF model is sensitive to the range of communication (in meters) rather than the number of cars ahead. On the other hand, even only five cars are enough to produce safe behavior for an accident scenario.

The inclusion of signal response delay negatively impacted the acceleration of automatic vehicles as seen in Table 4.4. When the vehicles receive a signal response with a delay (e.g., 0.1-sec), the acceleration of the vehicle is reduced, and vehicles maintain a "careful" behavior. Thus, the number of conflicts is reduced when the response delay is increased. For TTC $\leqslant$ 3.0 at a 50% market penetration rate, the average number of conflicts is reduced by approximately 11% for case-1, 20% for case-2, and 21% for case-3, respectively. Because the vehicle starts to move with reduced acceleration, the average delay starts to increase. The maximum average delay difference is recorded to 0.9 sec for case-3 at a 70% market penetration rate.

For the impact of multiple lanes, the lane-change conflicts for aggressive behavior are more severe for higher TTC values. The mobility benefits, such as average travel time, average delay, and others, have less significance for different "back" and "front" distance values. Table 4.4 shows that cautious behavior is suitable for the multilane CACF model.

Table 4.4 Summary of sensor network system optimization of the CACF model

Optimizing system parameters	Mobility	Safety
Impact of acceleration coefficients on safety	-	The acceleration coefficient of distance "kd" is most influential to network safety. Number of conflicts are increased for higher kd values.
Impact of V2I communication range on safety		A communication range from 200 to 250 meters is suitable for the CACF model.
Impact of communication signal response delay on safety and mobility	Because the vehicle starts to move with reduced acceleration, the average delay starts to increase. The maximum average delay difference is recorded to 0.9 sec for case-3 at a 70% market penetration rate.	The inclusion of signal response delay negatively impacted the acceleration of automatic vehicles and vehicle maintains a "careful" behavior. For TTC $\leq$ 3.0 at a 50% market penetration rate, the average conflicts are reduced by approximately 11% for 0.1 sec delay, 20% for 0.2 sec delay, and 21% for 0.3 sec delay.
Safety performance of CACF model for multi-lane logic	-	The CACF cautious lane-change and VISSIM default lane-change perform safer as compared with CACF aggressive model.

Note: The blank fields show insignificance either for mobility or safety analysis. Hence, no analyses are performed accordingly

5. CURRICULA AND EDUCATIONAL DEVELOPMENT

This project has trained 11 graduate students, including five master's students (Liuqing Hu, Hafiz Ahmad, Xinyi Yang, Salman Ahmad, and Tofatun Jannat) and six Ph.D. students (Zhiming Zhang, Mohanad Alshandah, Xinyi Yang, Yihao Ren, Leonard Chia, and Dawei Zhang). Among the 11 graduate students, two female students (Xinyi Yang and Tofatun Jannat), three master's students (Liuqing Hu, Hafiz Ahmad, and Xinyi Yang), and two Ph.D. students (Zhiming Zhang and Mohanad Alshandah) graduated with dissertations acknowledging this project. Additionally, this project also provided training to 18 undergraduate researchers. Among these undergraduate researchers, five are female and one is Native American. In summer 2020, this project also provided training for two Fargo high school teachers, Joshua Rogers from Davis High and Martha Nelson from North High. Based on this project, the teachers will develop high school course modules, which will be taught to an average of 20 high school students annually.

In addition, this project also partially supported various outreach activities for underrepresented students, such as female students, minority refugee minors, and Native American students. Specifically, there are four different outreach activities:

1) In October 2018 and 2019, this project partially supported a BrainSTEM Workshop which was offered to more than 60 middle school students.
2) Between January and April 2018 and 2019, this project also partially supported the CORE Outreach Program, which collaborates with CHARISM (a neighborhood support center for low-income families, and the Society of Women Engineers (SWE, a society to promote STEM to young girls) to promote engineering to young minority generations. It offered an eight-week workshop every year at four different Fargo centers (Carl Ben: 20 middle school students; Ed Clapp: 22 elementary students; Lewis and Clark: 22 elementary students; and McCormick: 35 elementary students) every Thursday afternoon to underserved youth, including low-income families, refugees, and young girls. These activities were held from 3 pm to 5:30 pm each Thursday for seven weeks.
3) From 2017 to 2020, this project also participated in the annual NATURE NDSU Summer Camp, held in June for an average of 22 Native American high school graduates and tribal college attendees every year.
4) From October to December 2022, this project also partially supported the NATURE SUNDAY Academy by offering a one-day Sunday camp for Native American high school students at the five different tribal sites (Turtle Mountain Community College, Sitting Bull College, Cankdeska Cikana Community College, Nueta Hidatsa Sahnish College, and United Tribes Technical College) with an average enrollment of 20 students at each tribal site (total ~100 students each year) with fully developed new interactive and hands-on lesson plans.

6.   SUMMARY AND FUTURE RESEARCH

This project developed an infrastructure support system based on infrastructure sensors and a new V2I algorithm for AVs to effectively use the infrastructure support system for enhanced safety and mobility. The infrastructure support system can monitor various vehicle and road condition data, including vehicle speed, wheelbase distances, the number of axles, vehicle classification, WIM, road roughness, and in-pavement cracks. With the real-time information from the infrastructure support system, the new CACF model developed can significantly improve the mobility and safety of the transportation system with different penetration rates of AVs. Specifically, the following conclusions can be drawn:

1) This study proposed an infrastructure support system layout that can be used to collect traffic and road condition data through in-pavement sensors, which can accurately estimate the speed and the wheelbase with an accuracy above 98%, classify vehicles with an accuracy of more than 96%, measure WIM with accuracies of 86.3% and 89.5% at 5 mph and 45 mph vehicle speeds, respectively, and measure road roughness and cracks with an estimated accuracy higher than 85%.
2) The newly developed CACF car-following model can use the monitored traffic and road conditions to enhance safety and mobility for AVs in mixed traffic environments. Microsimulation using VISSIM showed that the new CACF car-following model with real-time traffic and road condition updating can significantly improve the mobility and safety of the AVs.
3) The system optimization analysis showed that the sensor network will require a minimum V2I communication range of 300 meters with five vehicles or more in the network and a maximum communication delay of 10 seconds for the developed infrastructure support system.

This research will potentially contribute to the existing knowledge of vehicle and highway automation in which it uses the intelligent transportation system (ITS) application and implements it in a simulation platform. Effective communication between vehicles using the sensors embedded in the road infrastructure will ensure the safety of drivers by reducing the number of conflicts and crashes, improve travel times for different routes, and provide a tool for managing traffic congestion and traffic flows.

In the future, efforts will continue to increase the accuracy of the collected data from the sensors by testing the influencing factors measured from weather stations such as moisture, wind, etc. Those impact factors will also be applied to the developed model to increase the safety and mobility of the autonomous vehicle. The collected information includes number of axles, spacing between axles, gross weight, and minimum axle weight will be applied to Long-Term Pavement Performance (LTPP) classification rules and classify the vehicles with higher accuracy. Furthermore, the methodology of collecting the vehicular data from the sensors embedded on the roadways and importing it into the VISSIM software would be established. In addition, the proposed logic would expand to consider the functions of arterial and urban intersection networks i.e. an ego vehicle communicates with signalized junctions using V2I technology. Considering the average, minimum, and maximum speed are higher if the vehicles know the road quality based on the RIF (Yang et al. 2021) which are directly proportional with IRI, and the average RIF/IRI is around 0.95 (Bridgelall, 2013), RIF values will be added to the CACF model. Finally, the impacts of fuel efficiency and weather conditions on network optimization and safety would also be considered.

7. REFERENCES

Abou-Senna, H., Abdel-Aty, M., Wu, J., and Darius, B. (2015). "MRI-2: Integrated Simulation and Safety."

Aghabayk, K., Sarvi, M., and Young, W. (2015). "A state-of-the-art review of car-following models with particular considerations of heavy vehicles." *Transport Reviews*, *35*(1), 82-105.

Ahmed, H. U., Hu, L., Yang, X., Bridgelall, R., and Huang, Y. (2021). "Effects of smartphone sensor variability in road roughness evaluation." *International Journal of Pavement Engineering*, 1-6.

Alshandah, M., Huang, Y., Gao, J., Lu, P., and Tolliver, D. (2019). "Experimental crack detection in concrete pavement using point strain sensors." *2018 SPIE conference of smart structures and NDE*, Denver, CO, March 2019.

Alshandah, M., Huang, Y., Gao, Z., and Lu, P. (2020). "Internal crack detection in concrete pavement using discrete strain sensors." *Journal of Civil Structural Health Monitoring,* 10(2), 345-356.

Al-Tarawneh M., and Huang Y. (2017) "In-pavement fiber Bragg grating sensors for high-speed weigh-in-motion measurements*", 2017 SPIE conference of smart structures and NDE*, Portland, OR, March 2017.

Al-Tarawneh M., and Huang Y. (2018) "In-pavement fiber Bragg grating sensor for vehicle speed and wheelbase estimation*", 2018 SPIE conference of smart structures and NDE*, Denver, CO, March 2018.

Al-Tarawneh M., Huang, Y., Lu, P., and Tolliver, D. (2018). "Vehicle classification system using in-pavement fiber Bragg grating sensors." *IEEE Sensors Journal*, 18(7), 2807-2815.

Al-Tarawneh M., Huang, Y., Lu, P., and Bridgelall, R. (2019). "Weigh-In-Motion system in flexible pavements using fiber Bragg grating sensors part A: Concept." *IEEE Transactions on Intelligent Transportation Systems*, *21*(12), 5136-5147.

Antsaklis, P. J., Passino, K. M., and Wang, S. J. (1991). "An Introduction to Autonomous Control Systems." *IEEE Control Systems*, 11 (4): 5–13.

Bajwa, R., Rajagopal, R., Varaiya, P., and Kavaler, R. (2011). "In-pavement wireless sensor network for vehicle classification." *10th ACM/IEEE International Conference on Information Processing in Sensor Networks,* 85-96.

Bando, M., Hasebe, K., Nakayama, A., Shibata, A., and Sugiyama, Y. (1995). "Dynamical model of traffic congestion and numerical simulation." *Physical Review E*, *51*(2), 1035.

Bierstedt, J., Gooze, A., Gray, C., Peterman, J., Raykin, L., and Walters, J. (2014). "Effects of next-generation vehicles on travel demand and highway capacity." *FP Think Working Group*, 8, 10-1.

Brackstone, M., and McDonald, M. (1999). "Car-following: a historical review." *Transportation Research Part F: Traffic Psychology and Behaviour*, *2*(4), 181-196.

Bridgelall, R. (2013). "Connected vehicle approach for pavement roughness evaluation." *Journal of Infrastructure Systems*, 20(1), 04013001.

Broggi, A., Cappalunga, A., Caraffi, C., Cattani, S., Ghidoni, S., Grisleri, P., Paolo Porta, P., M. P. Posterli, Zani., and Beck, J. (2008). "The passive sensing suite of the TerraMax autonomous vehicle, " *In 2008 IEEE Intelligent Vehicles Symposium*, pp. 769-774, 2008.

Bushman, R., and Pratt, A. J. (1998). "Weigh in motion technology-economics and performance." *Presentation on the North American Travel Monitoring Exhibition and Conference (NATMEC). Charlotte*, North Carolina,

Caragliu, A., Del Bo, C., and Nijkamp, P. (2011). "Smart cities in Europe." *Journal of Urban Technology*, *18*(2), 65-82.

Chen, J., Liu, R., Ngoduy, D., and Shi, Z. (2016). "A new multi-anticipative car-following model with consideration of the desired following distance." *Nonlinear Dynamics*, *85*(4), 2705-2717.

Chen, S., Hu, J., Shi, Y., Peng, Y., Fang, J., Zhao, R., and Zhao, L. (2017). "Vehicle-to-everything (V2X) services supported by LTE-based systems and 5G." *IEEE Communications Standards Magazine*, *1*(2), 70-76.

Chen, Z., Pears, N., Freeman, M., and Austin, J. (2009). "Road vehicle classification using support vector machines." *2009 IEEE International Conference on Intelligent Computing and Intelligent Systems*.

Committee, S.O.-R.A.V.S. (2018). "Taxonomy and definitions for terms related to driving automation systems for on-road motor vehicles." *SAE International*: Warrendale, PA, USA.

Craig, J. L., Fraser, J. L., and Campos, J. (2017). "USDOT vehicle-to-pedestrian research: white paper."

Deakin, M. (2013). "From intelligent to smart cities," In "Smart Cities: Governing, Modelling and Analysing the Transition." *Taylor and Francis*.

Department of Transportation. (2017) "U.S. Department of Transportation Designates 10 Automated Vehicle Proving Grounds to Encourage Testing of New Technologies." https://www.transportation.gov/briefing-room/dot1717

Doi S. (2004). "Non-uniformity Compensation for Fiber Optic Weigh-in-motion Sensor." Florida Institute of Technology, 2004.

Fagnant, D. J., and Kockelman K. (2015). "Preparing a nation for autonomous vehicles: Opportunities, barriers and policy recommendations." *Transportation Research Part A: Policy and Practice*, 77, 167-181.

Fellendorf, M., and Vortisch, P. (2010). "Microscopic traffic flow simulator VISSIM." In *Fundamentals of Traffic Simulation* (pp. 63-93). Springer.

Forslöf, L. and Jones, H. (2015). "Roadroid: Continuous road condition monitoring with smart phones." *Journal of Civil Engineering and Architecture*, 9(4), 485-496.

Fyfe, M. R. (2016). "Safety evaluation of connected vehicle applications using micro-simulation." University of British Columbia.

Gehrig, S. K., and Stein, F. J. (1999). "Dead reckoning and cartography using stereo vision for an autonomous car." *IEEE/RSJ International Conference on Intelligent Robots and Systems*, 3, 1507-1512.

Greenblatt, N. A. (2016). "Self-driving cars and the law." *IEEE spectrum*, 53(2), 46-51.

Gupta, M., Benson, J., Patwa, F., and Sandhu, R. (2020). "Secure V2V and V2I communication in intelligent transportation using cloudlets." *IEEE Transactions on Services Computing*.

Hallenbeck, M. E., Selezneva, O. I., and Quinley, R. (2014). "Verification, refinement, and applicability of long-term pavement performance vehicle classification rules."

Harding, J., Powell, G., Yoon, R., Fikentscher, J., Doyle, C., Sade, D., Wang, J. (2014). "Vehicle-to-vehicle communications: readiness of V2V technology for application." *National Highway Traffic Safety Administration*, United States.

Harlow, C., and Peng, S. (2001). "Automatic vehicle classification system with range sensors." *Transportation Research Part C: Emerging Technologies*, *9*(4), 231-247.

Hollands, R. G. (2008). "Will the real smart city please stand up? Intelligent, progressive or entrepreneurial?" *City*, *12*(3), 303-320.

Huang, F., Liu, P., Yu, H., and Wang, W. (2013). "Identifying if VISSIM simulation model and SSAM provide reasonable estimates for field measured traffic conflicts at signalized intersections." *Accident Analysis and Prevention*, *50*, 1014-1024.

Huang, Y. H. (1993). "Pavement analysis and design."

Kato, T., Ninomiya, Y., and Masaki, I. (2002). "Preceding vehicle recognition based on learning from sample images." *IEEE Transactions on Intelligent Transportation Systems*, 3(4), 252-260.

Kim, D.-H., and Kwak, J. (2016). "Data transmission method for secure v2n communication." *International Information Institute (Tokyo). Information*, *19*(2), 481.

Komninos, N. (2011). "Intelligent cities: Variable geometries of spatial intelligence." *Journal of Intelligent Buildings International: From Intelligent Cities to Smart Cities*, 3, 172-188.

Kyriakidis, M., Happee, R., and De Winter, J. C. F. (2015). "Public opinion on automated driving: Results of an international questionnaire among 5,000 respondents." *Transportation Research Part F: Traffic Psychology and Behaviour*, 32, 127-140.

Laugier C. (1998). "Towards Autonomous Vehicles for Future Intelligent Transportation Systems." http://citeseerx.ist.psu.edu/viewdoc/download?doi=10.1.1.52.4080andrep=rep1andtype=pdf

Lee, B. (2003). "Review of the present status of optical fiber sensors." *Optical Fiber Technology*, *9*(2), 57-79.

Leech, J., Whelan, G., Bhaiji, M., Hawes, M., and Scharring, K. (2015). "Connected and autonomous vehicles-the UK economic opportunity". *KPMG*.

Lenz, H., Wagner, C., and Sollacher, R. (1999). "Multi-anticipative car-following model." *The European Physical Journal B-Condensed Matter and Complex Systems*, *7*(2), 331-335.

Litman, T. (2017). "Autonomous vehicle implementation predictions." Victoria, Canada: Victoria Transport Policy Institute.

Liu, R., Chen, X., Li, J., Guo, L., and Yu, J. (2006). "Evaluating Innovative Sensors and Techniques for Measuring Traffic Loads." *Final Project Report, TxDOT Project 0-4509*.

Loprencipe, G., & Zoccali, P. (2017). "Use of generated artificial road profiles in road roughness evaluation." *Journal of Modern Transportation*, 25(1), 24-33.

Madevska-Bogdanova, A., Nikolik, D., and Curfs, L. (2004). "Probabilistic SVM outputs for pattern recognition using analytical geometry." *Neurocomputing*, *62*, 293-303.

Majumder, M., Gangopadhyay, T. K., Chakraborty, A. K., Dasgupta, K., and Bhattacharya, D. K. (2008). "Fiber Bragg gratings in structural health monitoring—Present status and applications." *Sensors and Actuators A: Physical*, *147*(1), 150-164.

Malla, R. B., Sen, A., and Garrick, N. W. (2008). "A special fiber optic sensor for measuring wheel loads of vehicles on highways." *Sensors*, *8*(4), 2551-2568.

Marcondes, J., Burgess, G. J., Harichandran, R., and Snyder, M. B. (1991). "Spectral analysis of highway pavement roughness." *Journal of Transportation engineering*, 117(5), 540-549.

Massaroni, C., Saccomandi, P., and Schena, E. (2015). "Medical smart textiles based on fiber optic technology: an overview." *Journal of Functional Biomaterials*, *6*(2), 204-221.

McGhee, K. H. (2004). "Automated pavement distress collection techniques." *Transportation Research Board.*

Meller, S. A., De Vries, M. J., Arya, V., Claus, R. O., and Zabaronick, N. (1998). "Advances in optical fiber sensors for vehicle detection." *Intelligent Transportation Systems*.

Mendez, A. (2007). "Fiber Bragg grating sensors: a market overview." *Third European Workshop on Optical Fiber Sensors*.

Milanes, V., Villagrá, J., Godoy, J., Simó, J., Pérez, J., and Onieva, E. (2012). "An intelligent V2I-based traffic management system." *IEEE Transactions on Intelligent Transportation Systems*, *13*(1), 49-58.

Milanés, V., Shladover, S. E., Spring, J., Nowakowski, C., Kawazoe, H., and Nakamura, M. (2013). "Cooperative adaptive cruise control in real traffic situations." *IEEE Transactions on Intelligent Transportation Systems*, *15*(1), 296-305.

Mussa, R., Kwigizile, V., and Selekwa, M. (2006). "Probabilistic neural networks application for vehicle classification." *Journal of Transportation Engineering*, *132*(4), 293-302.

National Highway Traffic Safety Administration. (2008). "National motor vehicle crash causation survey: Report to congress." *National Highway Traffic Safety Administration Technical Report DOT HS, 811,* 059.

National Highway Traffic Safety Administration. (2013). "Preliminary statement of policy concerning automated vehicles." Washington, DC, 1, 14.

Nelson, B. N. (2001). "Automatic vehicle detection in infrared imagery using a fuzzy inference-based classification system." *IEEE Transactions on fuzzy Systems*, 9(1), 53-61.

Oh, H.-S., and Sim, J. (2004). "Interface debonding failure in beams strengthened with externally bonded GFRP." *Composite Interfaces*, *11*(1), 25-42.

Papadoulis, A., Quddus, M., and Imprialou, M. (2019). "Evaluating the safety impact of connected and autonomous vehicles on motorways." *Accident Analysis and Prevention*, *124*, 12-22.

Park, S., Kim, Y., Matson, E. T., and Smith, A. H. (2016). "Accessible synthetic aperture radar system for autonomous vehicle sensing, " In 2016 IEEE Sensors Applications Symposium (SAS0), pp. 1-6.

Paskaleva, K. (2009). "Enabling the smart city: The progress of e-city governance in Europe." *International Journal of Innovation and Regional Development*, 1 (4), 405-422.

PTV, A. (2020). *VISSIM 2020 User Manual.* In: PTV Karlsruhe, Karlsruhe, Germany.

Ramsey, M. (2015). "Self-Driving Cars Could Cut Down on Accidents, Study Says." *The Wall Street Journal*, 1425567905.

Schermers, G., Malone, K., and Van Arem, B. (2004). "Dutch Evaluation of Chauffeur Assistant (DECA): Traffic flow effects of implementation in the heavy goods vehicles sector." *ITS World Congress*, Nagoya, Aichi.

Schoettle, B. and Sivak, M. (2014). "A survey of public opinion about autonomous and self-driving vehicles in the U.S., the U.K., and Australia." *The University of Michigan Transportation Research Institute*, Report No. UMTRI-2014-21.

Scholkopf, B., Sung, K.-K., Burges, C. J., Girosi, F., Niyogi, P., Poggio, T., and Vapnik, V. (1997). "Comparing support vector machines with Gaussian kernels to radial basis function classifiers." *IEEE transactions on Signal Processing*, *45*(11), 2758-2765.

Selekwa, M. F., Kwigizile, V., and Mussa, R. N. (2005). "Setting up a probabilistic neural network for classification of highway vehicles." *International Journal of Computational Intelligence and Applications*, *5*(04), 411-423.

Shanker, R., Jonas, A., Devitt, S., Huberty, K., Flannery, S., Greene, W., ... and Humphrey, A. (2013). "Autonomous cars: Self-driving the new auto industry paradigm." *Morgan Stanley blue paper*, 1-109.

Simonite, T. (2013). "Data Shows Google's Robot Cars Are Smoother, Safer Drivers Than You or I." *MIT Technology Review.*

Sroka, R. (2004). "Data fusion methods based on fuzzy measures in vehicle classification process." *Proceedings of the 21st IEEE Instrumentation and Measurement Technology Conference*, 2234-2239.

Stanton, N. A., and Young, M. S. (2005). "Driver behaviour with adaptive cruise control." *Ergonomics*, *48*(10), 1294-1313.

Stenquist, P. (2014). "In Self-Driving Cars, a Potential Lifeline for the Disable." *The New York Times.*

Sukennik, P., and Group, P. (2018). "Micro-simulation guide for automated vehicles." *COEXIST (h2020-coexist. eu).*

Sun, C., Ritchie, S. G., and Oh, S. (2003). "Inductive classifying artificial network for vehicle type categorization." *Computer-Aided Civil and Infrastructure Engineering*, *18*(3), 161-172.

Sun, S.-h., Hu, J.-l., Peng, Y., Pan, X.-m., Zhao, L., and Fang, J.-y. (2016). "Support for vehicle-to-everything services based on LTE." *IEEE Wireless Communications*, *23*(3), 4-8.

Tang, Q., Dagley, G., Ghamsari, A., Price, M., and Hoover, J. (2020). "Automatic vehicle configuration based on sensor data." In: Google Patents.

Tientrakool, P., Ho, Y., and Maxemchuk, N. F. (2011). "Highway Capacity Benefits from Using Vehicle-to-Vehicle Communication and Sensors for Collision Avoidance." *Vehicular Technology Conference (VTC Fall), 2011 IEEE*, 12407267.

Udd, E., and Kunz, M. (2003). "Development and evaluation of fiber optic sensors". Oregon Department of Transportation.

U. S. Department of Transportation. (2016) "Federal Automated Vehicles Policy." National Highway Traffic Safety Administration.

U.S. Secretary of Transportation. "Beyond Traffic 2045." Final Report, U.S. DOT. https://www.transportation.gov/policy-initiatives/beyond-traffic-2045-final-report

Van Arem, B., Van Driel, C. J., and Visser, R. (2006). "The impact of cooperative adaptive cruise control on traffic-flow characteristics," *IEEE Transactions on intelligent transportation systems*, vol. 7, no. 4, pp. 429-436.

, B., De Vos, A., and Vanderschuren, M. J. (1997) "The microscopic traffic simulation model MIXIC 1.3.".

VanderWerf, J., Shladover, S., Kourjanskaia, N., Miller, M. (2002) "Effects of adaptive cruise control systems on highway traffic flow capacity," *Transportation Research Record,* vol. 1800, no. 1, pp. 78-84, Jan. 2002,

VanderWerf, J., Shladover, S., Kourjanskaia, N., Miller, M., and Krishnan, H. (2001). "Modeling effects of driver control assistance systems on traffic." *Transportation Research Record*, *1748*(1), 167-174.

Wierzba, P., and Kosmowski, B. (2000). "Polarimetric sensors for weigh-in-motion of road vehicles." *Optoelectronics Review*(2), 181-188.

Wu, J., Xu, H., Tian, Y., Zhang, Y., Zhao, J., and Lv, B. (2020). "An automatic lane identification method for the roadside light detection and ranging sensor." *Journal of Intelligent Transportation Systems*, *24*(5), 467-479.

Yang, X., Ren, Y., Hu, L., Huang, Y., and Lu, P. (2021). "Evaluating the impact of road quality in driving behavior of autonomous vehicles." *In Sensors and Smart Structures Technologies for Civil, Mechanical, and Aerospace Systems 2021*,Vol. 11591, p. 1159106

Yang, X., Hu, L., Ahmed, H. U., Bridgelall, R., and Huang, Y. (2020). "Calibration of smartphone sensors to evaluate the ride quality of paved and unpaved roads." *International Journal of Pavement Engineering*, 1-11.

Younsi, M., Diaf, M., and Siarry, P. (2020). "Automatic multiple moving humans detection and tracking in image sequences taken from a stationary thermal infrared camera." *Expert Systems with Applications*, *146*, 113171.

Zhang, Z., Deng, F., Huang, Y., and Bridgelall, R. (2015a). "Road roughness evaluation using in-pavement strain sensors." *Smart Materials and Structures*, 24(11), 115029.

Zhang, Z., Huang, Y., Bridgelall, R., Palek, L., Strommen, R. (2015b) "Sampling optimization for high-speed weigh-in-motion measurements using in-pavement strain-based sensors." *Meas. Sci. Technol*, 26(6), 65003.

Zhang, Z., Huang, Y., Bridgelall, R., and Lu, P. (2017). "Optimal system design for weigh-in-motion measurements using in-pavement strain sensors." *IEEE Sensors Journal*, 17(23), 7677-7684.

Zhang, Z., Sun, C., and Huang, Y. (2019). "Sparse signal recovery for WIM measurements from undersampled data through compressed sensing." *Measurement*, 151, 107181.

Zhao, L., and Sun, J. (2013). "Simulation framework for vehicle platooning and car-following behaviors under connected-vehicle environment." *Procedia-Social and Behavioral Sciences*, 96, 914-924.